ACS OMEGA

Article

Cite This: ACS Omega 2019, 4, 22214−22227

http://pubs.acs.org/journal/acsodf

Folic Acid-Functionalized, Condensed Magnetic Nanoparticles for Targeted Delivery of Doxorubicin to Tumor Cancer Cells Overexpressing the Folate Receptor

Athina Angelopoulou,*[,†] Argiris Kolokithas-Ntoukas,[†,‡] Christos Fytas,[†] and Konstantinos Avgoustakis[†,§]

[†]Department of Pharmacy, School of Health Sciences and [‡]Department of Materials Science, School of Natural Sciences, University of Patras, Patras 26504, Greece

[§]Clinical Studies Unit, Biomedical Research Foundation Academy of Athens (BRFAA), 4 Soranou Ephessiou Street, Athens 11527, Greece

Supporting Information

ABSTRACT: This study concerns the development of folic acid (FA)-functionalized iron oxide condensed colloidal magnetic clusters for a more selective delivery of doxorubicin (DOX) to tumor cancer cells overexpressing the folate receptor. Alginate-coated condensed magnetic nanoparticles (co-MIONs) were synthesized via an alkaline precipitation method of an iron precursor in the presence of sodium alginate. Poly(ethylene glycol) (OH-PEG-NH_2) was conjugated to the carboxylic acid end group of alginate and folic acid (FA) was conjugated to the hydroxyl terminal group of PEG to produce folate-functionalized, pegylated co-MIONS (Mag-Alg-PEG-FA). The physicochemical properties of nanoparticles were fully characterized. DOX was loaded on the nanoparticles, and the cellular uptake and anticancer efficacy of the nanoparticles were examined in cancer cell lines expressing and not expressing the folate receptor. The biocompatibility of the carrier (blank nanoparticles) was also evaluated by cytocompatibility and hemocompatibility experiments. The nanoparticles exhibited sustained DOX release in aqueous buffers and biorelevant media, which was responsive to pH and external alternating current magnetic fields. The effect of the magnetic field on DOX percentage release appeared to be independent of the timing (onset time) of magnetic field application, providing flexibility to the magnetic control of drug release from the nanoparticles. The blank nanoparticles were not cytotoxic and did not cause hemolysis. The DOX-loaded and FA-functionalized nanoparticles exhibited increased uptake and caused increased apoptosis and cytotoxicity against the MDA-MB-231 cell line, expressing the folate receptor, compared to the MCF-7 cell line, not expressing the folate receptor. The application of a 0.5 T magnetic field during incubation of the nanoparticles with the cancer cells increased the cellular uptake and cytotoxicity of the nanoparticles. The obtained results indicate the potential of the folate-functionalized, pegylated co-MIONS for a more efficacious DOX delivery to cancer cells of solid tumors.

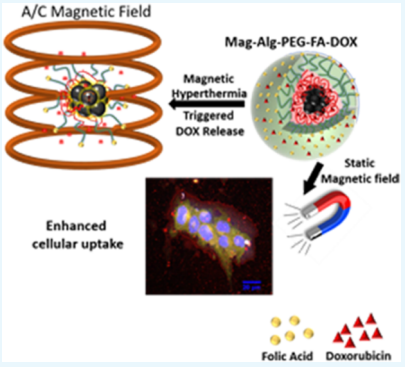

INTRODUCTION

Conventional cancer pharmacotherapy methods have several limitations, such as the lack of therapeutic efficacy, toxicity to healthy tissues, and the development of innate resistance of cancer cells to chemotherapeutic agents, especially in the environment of solid tumors.[1] The cellular environment of tumors is nowadays considered as the most determining factor that could contribute to the treatment of cancer.[1,2] Of particular interest is the addition of molecular targeting agents such as antibodies, peptides, folic acid (FA), etc. to nanosized delivery systems.[3−6] Such targeted and personalized systems use the molecular characteristics of the cancer cells of the tumor and its microenvironment to provide increased drug accumulation in the tumor area and targeted and controlled release of the drug, thereby reducing toxicity and thus improving the benefit/risk profile for patients.[3−6]

Among the various forms of cancer, a particularly aggressive and rapidly growing form is solid tumors, the majority of which overexpress the folic acid receptor, such as the ovary, kidney, lung, brain, endometrium, pancreas, stomach, prostate, testicle, bladder, head and neck, breast, and non-small-cell lung cancers.[3] Folic acid (FA) is absolutely essential for the synthesis, repair, and methylation of DNA, as well as the metabolism of amino acids and RNA. Therefore, its role is essential for cell growth, proliferation, and survival, which signifies its particular importance in the development and maintenance of cancer cells.[3] Of the four known folate receptor isoforms (folate receptors α, β, γ, and d), FRα and FRβ are present in the plasma membrane and bind folic acid with the

Received: October 25, 2019
Accepted: November 25, 2019
Published: December 9, 2019

DOI: 10.1021/acsomega.9b03594
ACS Omega 2019, 4, 22214−22227

Table 1. Physicochemical Characteristics of Magnetic Nanoparticles

	diameter (nm)	polydispersity index (PDI)	ζ-potential (mV)	loading capacity (%) for DOX or rhodamine
Mag-Alg	75 ± 1.31	0.137 ± 0.025	−51.1 ± 3.87	
Mag-Alg-PEG	97.5 ± 0.42	0.106 ± 0.013	−1.99 ± 0.44	
Mag-Alg-PEG-FA	95.19 ± 0.26	0.093 ± 0.013	−22.1 ± 0.76	
Mag-Alg-PEG-FA/DOX	97.12 ± 0.76	0.111 ± 0.023	−0.57 ± 0.03	10.47 ± 0.44
Mag-Alg-PEG-FA/rhodamine	91.81 ± 0.38	0.095 ± 0.011	−1.15 ± 0.15	3.06 ± 0.91

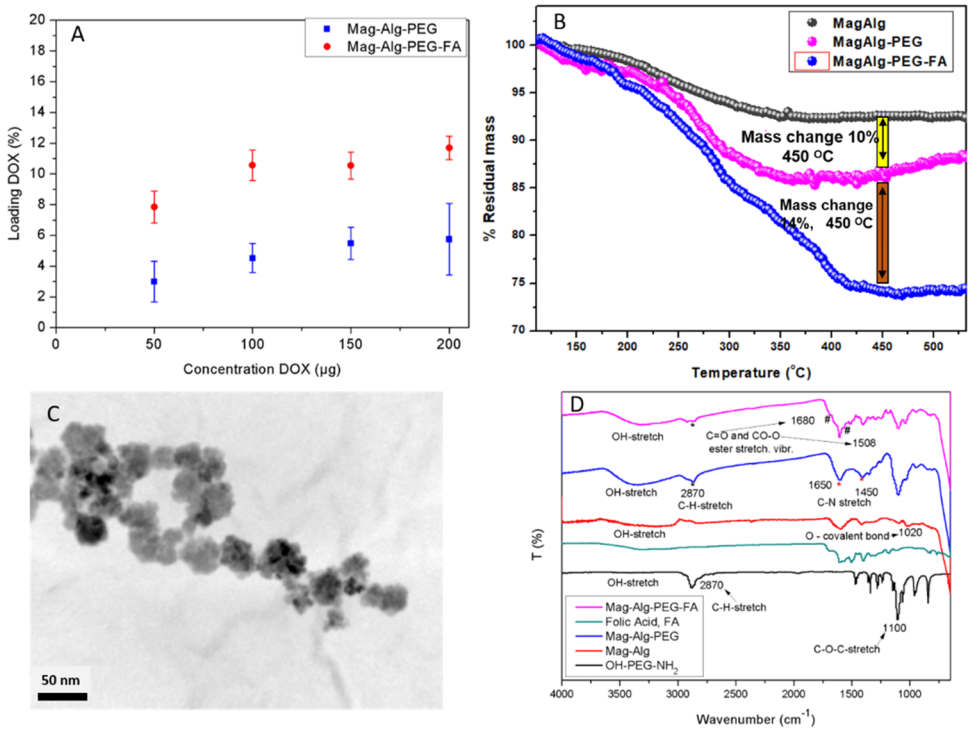

Figure 1. Loading capacity, TGA curves, TEM images, and ATR spectra of the magnetic nanoparticles. (A) Loading capacities of Mag-Alg-PEG and Mag-Alg-PEG-FA nanoparticles at initial DOX amounts (feed) of 50, 100, 150, and 200 μg. (B) TGA curves of Mag-Alg (black circles), Mag-Alg-PEG (magenta circles), and Mag-Alg-PEG-FA nanoparticles (light-blue circles). The mass change noted (yellow bar and orange bar) refers to the residual mass difference between the Mag-Alg/Mag-Alg-PEG and the Mag-Alg-PEG/Mag-Alg-PEG-FA curves at 450 °C. (C) Typical TEM images from the Mag-Alg-PEG-FA nanoparticles. (D) ATR spectra of Mag-Alg-PEG-FA nanoparticles (magenta line), folic acid (cyan line), Mag-Alg-PEG nanoparticles (blue line), Mag-Alg nanoparticles (red line), and OH-PEG-NH_2 (black line). Alg: alginate; Mag: magnetic; FA: folic acid; TEM: transmission electron microscopy; TGA: thermogravimetric analysis.

highest affinity. Cells expressing FRα are more efficient in absorbing folic acid, since FRα binds folic acid with a binding affinity of 0.34 nM.[3,4] In normal tissues and organs, the expression of FRα is restricted to only certain regions, which include the kidneys, lungs, choroid membrane, and placenta, where FRα is restricted and cannot come into contact with folic acid molecules administered intravenously, such as folic acid molecules bound to a targeted delivery system administered intravenously.[3,4] Studies have shown that in solid tumor environments, cancer cells exhibit high levels of FRα receptor expression, where this overexpression is associated with advanced stage disease and is a negative prognostic factor for breast, colon, endometrium, and ovarian cancers.[3−5] Therefore, the FRα receptor is considered to be a particularly important therapeutic target, as it can provide an effective option for targeted cancer treatment through the development of folic acid-modified nanostructures for the selective transfer of anticancer drugs to FR-overexpressing cancer cells.[6]

An important application for the development of targeted delivery systems is provided by magnetic iron oxide nanoassemblies (MIONs), which have attracted significant research interest as they can provide both imaging and selective drug delivery capabilities.[6−13] The use of magnetically targeted nanoparticles, whose biological behavior (biodistribution) can be controlled by the application of external magnetic fields, is a particularly interesting combinatorial approach to molecular targeting for the development of selective therapies. In essence, magnetic nanoparticles are state-of-the-art technology in the field of drug delivery since they can be modified with biocompatible polymers and biopolymers (poly(ethylene glycol) (PEG), cellulose, and alginic acid), carry molecular targeting agents and/or probe molecules (fluorescent labels), and simultaneously be imaged by magnetic resonance imaging (MRI).[6−9]

Colloidal magnetic nanocrystals can be grown in dense order with their nanocrystals arranged so that their crystalline planes adopt the same orientation through epitaxial aggregation. These condensed magnetic nanoparticles (co-MIONs) have significant advantages. They exhibit dramatically increased magnetic response compared to conventional magnetic nanocrystals, making them more effective in magnetic targeting

DOI: 10.1021/acsomega.9b03594
ACS Omega 2019, 4, 22214−22227

Scheme 1. Graphic Representation of the Functionalization of Mag-Alg-PEG-FA Magnetic Nanoparticles

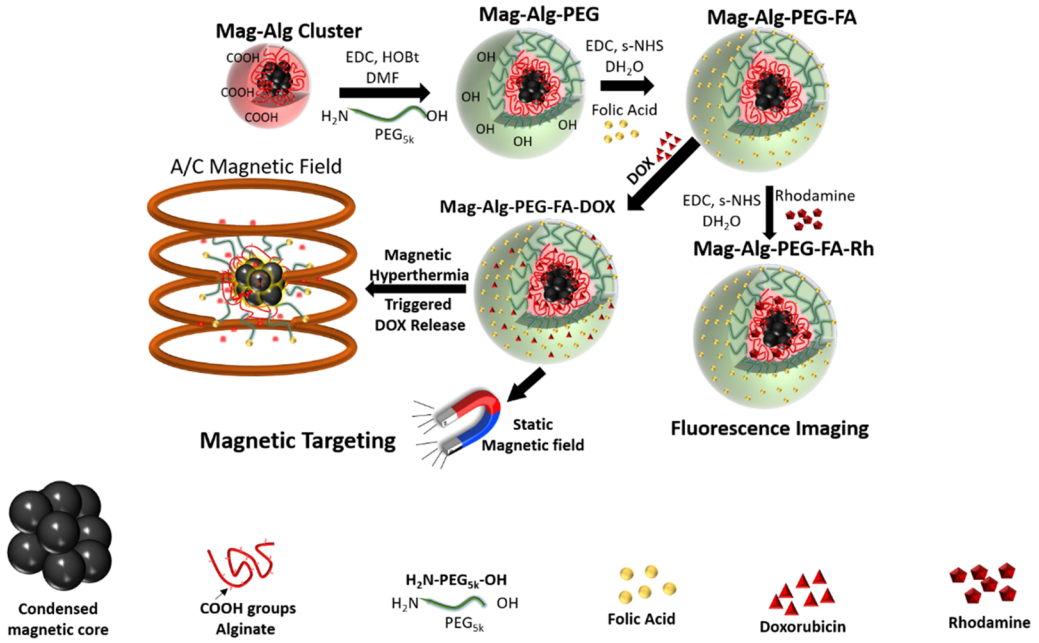

applications and magnetic resonance imaging (MRI).[7,8] Thus, co-MIONs have the ability to entrap a large number of magnetic nanocrystals, which are in close contact with each other, displaying excellent magnetic properties.[7,8] In recent studies of our group,[7,8] the development of co-MIONs from a single ferrous molecular precursor in the presence of alginate (alginate, Alg) at low temperature was achieved. These colloidally dense co-MIONs exhibited a better response when applied to an external static magnetic field, while the presence of alginate proved to be crucial for the epitaxial aggregation of the nanocrystals in the core. In addition, the alginate shell enabled the efficient loading with drug and the functional modification of the nanoparticles, e.g., the binding of poly(ethylene glycol) (PEG) molecules capable of imparting desired properties to the particles, such as increased blood-circulating properties after intravenous administration.[8] Nevertheless, these pegylated co-MIONs still lack the potential for specific interaction with the cancer cells of the tumors, reducing their potential to deliver the drug they carry selectively to the cancer cells and limiting, consequently, their therapeutic potential. These co-MION nanosystems could, thus, be significantly improved through further functional modification to possess molecular targeting ability for the cancer cells through receptor−ligand interaction and the ability to selectively release the drug in the extracellular and intracellular environments of cancer cells. Thus, in this work, the pegylated, alginate co-MIONS were further developed by their functional modification with molecular targeting units (folic acid molecules) for the targeting of tumor cancer cells overexpressing folic acid receptors. In addition, PEG with a molecular weight (5000) higher than previously used[8] was selected with the aim to increase the efficiency of pegylation to stabilize the alginate co-MIONS. The Mag-Alg-PEG-FA co-MIONS were loaded with the chemotherapeutic drug doxorubicin (DOX). These folate-functionalized, doxorubicin-loaded co-MIONs are expected to accumulate in the tumor area by applying an external magnetic field at the tumor area and due to the enhanced permeability and retention (EPR) effect.[11] These, due to the FA units present on their surface, would provide a more selective delivery of the chemotherapeutic drug (DOX) to the cancer cells overexpressing FA receptors. The developed DOX-loaded Mag-Alg-PEG-FA co-MIONS were characterized by their physicochemical characteristics (size and ζ-potential), colloidal stability, and ability to load and release the drug. The release of the drug was studied at different pH values (blood pH 7.4 and an acidic pH 6.0, representing the acidic tumor environment) and in different biological media [Roswell Park Memorial Institute (RPMI) 1640 medium[14] and blood plasma[15]], as well as under hyperthermia in a specific magnetic fluid hyperthermia (MFH) device. Optimal nanoparticle compositions were studied for their anticancer activity and their intracellular localization in human cancer cell lines expressing and not expressing (for comparison) the FRα receptor.

RESULTS

Characterization of the Synthesized Nanoparticles. The maximum loading capacity of Mag-Alg-PEG-FA co-MIONS with DOX was 10.47% (w/w) (Table 1). The loading capacity with DOX was higher in the case of Mag-Alg-PEG-FA co-MIONS than in the case of Mag-Alg-PEG co-MIONS (Figure 1A). The initial DOX feed (50, 100, 150, and 200 μg/mL) did not affect the basic physicochemical characteristics (size and ζ-potential) of the Mag-Alg-PEG-FA nanoparticles (see Supporting Information (SI) Figure S1). The Mag-Alg nanoparticles exhibited an average size (hydrodynamic diameter) of 75 nm, which increased slightly after pegylation (Mag-Alg-PEG nanoparticles) to 97.5 nm and did not change significantly when FA was conjugated on the nanoparticles (Mag-Alg-PEG-FA). The ζ-potential of the Mag-Alg nanoparticles was negative (−51 mV), due to the negatively charged groups of the magnetic core (Fe−O$^-$) and the carboxylate groups (−COO$^-$) of alginate (Alg). Upon nanoparticle pegylation, the ζ-potential of Mag-Alg-PEG approached neutrality (−2 mV), due to the reduction in the number of free carboxylic acid groups in alginate. After FA conjugation on

DOI: 10.1021/acsomega.9b03594
ACS Omega 2019, 4, 22214−22227

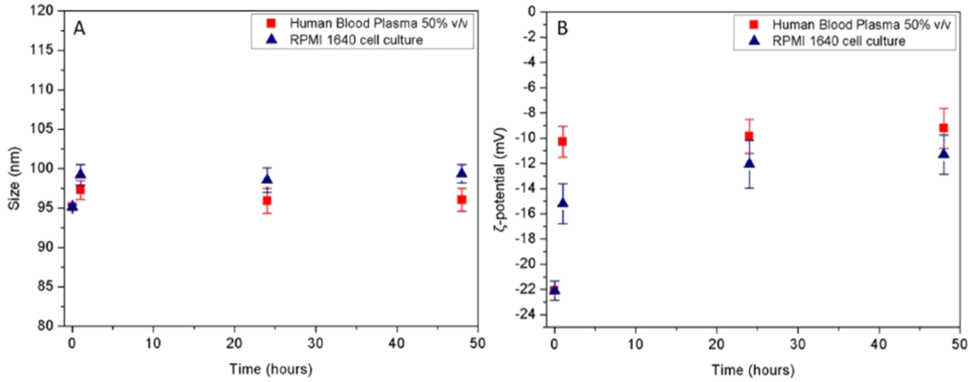

Figure 2. Evaluation of the colloidal stability of Mag-Alg-PEG-FA nanoparticles. (A) Average size and (B) ζ-potential change upon 48 h incubation of the Mag-Alg-PEG-FA nanoparticles in RPMI-1640 cell culture medium and human blood plasma (diluted 50% v/v).

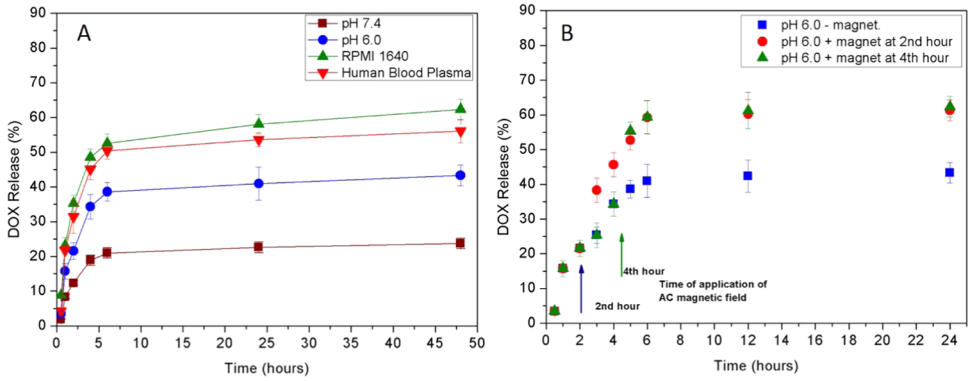

Figure 3. In vitro drug release from the Mag-Alg-PEG-FA nanoparticles. (A) Release profiles of DOX from the magnetic nanoparticles in phosphate-buffered saline with pH 7.4 and 6.0, RPMI-1640, and human blood plasma (10% v/v). (B) DOX release from the magnetic nanoparticles when an alternating current (AC) magnetic field (f = 110.6 kHz, B = 25 mT, I = 12.2 A, V = 28.3 V) was applied for 15 min at the beginning of the second (dark-blue circles) or at the beginning of the fourth hour (olive circles).

the pegylated nanoparticles, the ζ-potential of Mag-Alg-PEG-FA nanoparticles again assumed negative values (−22 mV), due to the remaining free carboxylic acid groups ($-COO^-$) of FA (Scheme 1). The successful functionalization of the nanoparticles was confirmed by attenuated total reflection (ATR) spectroscopy (Figure 1D). The presence of PEG in Mag-Alg-PEG nanoparticles was indicated by the presence of characteristic stretching vibration bands in the PEG chain at 2870 cm^{-1} (C−H stretch vibration) and in the range 1300−1200 cm^{-1} (C−O−C stretch vibration) and by the presence of N−H out-of-plane stretching vibrations in the range 770−970 cm^{-1}. The conjugation of PEG on the Mag-Alg surface was further supported by the distinct C−N stretching vibration bands of amide bonding at 1650 and 1450 cm^{-1}. As for Mag-Alg-PEG-FA nanoparticles, the successful FA conjugation on the hydroxyl (−OH) terminal group of the PEG chain by an ester linkage was confirmed from the presence of peaks at 1680 and 1508 cm^{-1}, corresponding to the stretching vibration bands of C═O and CO−O ester, respectively.[12,13] Detailed ATR characterization is provided in SI Figure S2.

Thermogravimetric analysis (TGA) was implemented for the parent Mag-Alg and after every step of conjugation for the Mag-Alg-PEG and Mag-Alg-PEG-FA nanoparticles, under a N_2 stream, and the curves of mass change versus temperature obtained are shown in Figure 1B. The observed mass changes in TGA of the magnetic nanoparticles were due to the decomposition of the organic material (alginate, alginate-PEG, or alginate-PEG-folate). The thermograms indicated a mass loss of 10% (w/w) due to alginate decomposition, a 12% (w/w) loss due to PEG decomposition, and a further 13% (w/w) loss due to FA decomposition. Taking this into consideration, the composition (w/w) of the here-synthesized Mag-Alg-PEG-FA co-MIONS is 65% iron oxide, 10% alginate, 12% PEG, and 13% FA.

The structural characteristics of the magnetic nanoparticles were also elucidated by transmission electron microscopy (TEM) analysis (Figure 1C). TEM micrographs indicated the structural organization of the nanoparticles forming clusters of densely packed magnetic nanoparticles.[7] The mean cluster size was around 40−50 nm. As expected, the polymeric surface of Alg-PEG-FA surrounding the magnetic nanoparticles could not be observed in TEM micrographs, due to the high contrast of the crystalline planes of magnetic nanocrystallites.[7,13]

Colloidal Stability of Magnetic Nanoparticles. Preliminary experiments indicated that the use of a higher-molecular-weight PEG (5000) resulted in the higher stability of the alginate co-MIONS in diluted blood plasma compared to a lower-molecular-weight PEG (2000) used previously[8] (SI Figure S3) and therefore a PEG (5000) was selected in this study. The average hydrodynamic diameter of Mag-Alg-PEG-FA nanoparticles remained essentially stable, and the nanoparticles did not aggregate upon incubation up to 48 h in RPMI-1640 medium and diluted human blood plasma (50% v/v) (Figure 2A). The average ζ-potential of the nanoparticles became less negative when they were transferred to the biorelevant media, −10 and −15 mV in plasma and RPMI-

DOI: 10.1021/acsomega.9b03594
ACS Omega 2019, 4, 22214−22227

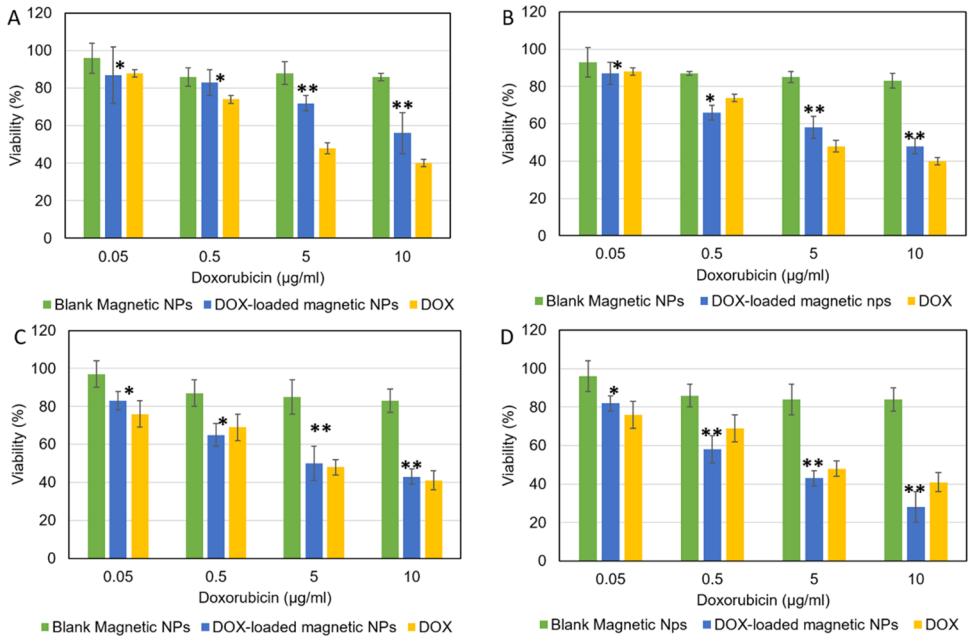

Figure 4. Cytotoxicities of free DOX, blank Mag-Alg-PEG-FA nanoparticles, and DOX-loaded Mag-Alg-PEG-FA nanoparticles on (A, B) MCF-7 cells and (C, D) MDA-MB 231 after 24 h of incubation (A, C) in the absence and (B, D) in the presence of an external magnetic field. Asterisks indicate the statistical significance of the difference between results obtained for DOX-loaded nanoparticles and free DOX (*$p < 0.05$, **$p < 0.005$). The concentrations of blank nanoparticles in the graphs are 0.43, 4.34, 43.48, and 86.9 μg/mL and correspond to the concentrations of DOX-loaded nanoparticles used to generate the DOX concentrations mentioned in the graphs (0.05, 0.5, 5, and 10 μg/mL, respectively).

1640, respectively, compared to −22 mV in water. With increased incubation time, the ζ-potential of the nanoparticles was stabilized at values around −9 and −12 mV in plasma and RPMI-1640, respectively (Figure 2B). Probably, the interaction of the nanoparticles with cationic constituents of the biorelevant media resulted in the neutralization of a part of the negative surface charges of the nanoparticles, leading to less negative ζ-potential values in these media compared to water (Figure 2B); however, this interaction did not result in nanoparticle aggregation even after a prolonged incubation period of 48 h (Figure 2A).

In Vitro DOX Release from the Nanoparticles. DOX release from the Mag-Alg-PEG-FA nanoparticles in phosphate-buffered saline (PBS) (pH 7.4) was about 23% at 48 h, while the release in PBS (pH 6.0) was 43% in the same time period. At acidic pH, owing to the reduction of the number of negatively charged carboxylate groups,[16] a decrease in the electrostatic interaction between DOX molecules (positively charged) and the alginate backbone[17] is expected, which in combination with the increased solubility of protonated DOX[18,19] results in the higher release of DOX in the acidic aqueous environment (Figure 3A). An increased release rate relatively to pH 7.4 buffer was observed in the biorelevant media. Thus, DOX release at 48 h reached 56% in human blood plasma (10% v/v) and 62% in RPMI-1640 [with fetal bovine serum (FBS) 10% v/v] (Figure 3A), probably due to the intervention of media constituents, such as proteins, in drug−carrier interactions. To quantify the kinetics of DOX release, it was supposed that drug release followed first-order kinetics and the release data were fitted to first-order kinetics. The fitting provided release constants of 0.011 and 0.036 h^{-1} for the release in PBS with pH 7.4 and 6.0, respectively. In the case of human blood plasma and RPMI-1640, the release constants were 0.049 and 0.054 h^{-1}, respectively. Although the release values were low, especially in pH 7.4, for precise release kinetics analysis, the values of the release rate constants obtained indicated the significantly higher rate (5-fold) of DOX release in the biorelevant media.

The application of an AC magnetic field during DOX release at pH 6.0 resulted in an increased release rate compared to the release in the absence of the magnetic field (Figure 3B). The magnetic field was applied for 15 min (total time) at different time periods of the release experiments, specifically for 15 min at the beginning of the second or for 15 min at the beginning of the fourth hour. Similar release values of around 60% in 6 h were obtained in both cases (Figure 3B).

In Vitro Cytotoxicity. The viability of MCF-7 and MDA-MB 231 human breast adenocarcinoma cancer cell lines was investigated after a 24 h incubation with Mag-Alg-PEG-FA nanoparticles. At all examined concentrations (0.43−86.9 μg/mL), the blank (without the drug) nanoparticles resulted in high cell viability (above 80%) with both cell lines (Figure 4). The DOX-loaded nanoparticles exhibited dose-dependent cytotoxicity against the MCF-7 and MDA-MB 231 cell lines (Figure 4). Moreover, the DOX-loaded nanoparticles exhibited lower cytotoxicity than free DOX against MCF-7 cells (Figure 4A) and similar cytotoxicity with free DOX against MDA-MB 231 cells (Figure 4C). When a 0.5 T magnetic field gradient was applied to the cells, the DOX-loaded Mag-Alg-PEG-FA nanoparticles exhibited lower or similar cytotoxicity ($p < 0.05$) compared to free DOX against the MCF-7 cells (Figure 4B) but higher ($p < 0.05$) cytotoxicity than free DOX against the MDA-MB 231 cells (Figure 4D). The IC_{50} values of DOX-loaded nanoparticles and free DOX are presented in Table 2 for both cell lines. The nanoparticles exhibited lower IC_{50} values against the MDA-MB 231 cells compared to the MCF-7 cells, both with and without the application of a magnetic field gradient. The IC_{50} values of free DOX are lower in MCF-7 cells compared to the DOX-loaded nanoparticles, especially without the application of a magnetic field gradient, whereas

DOI: 10.1021/acsomega.9b03594
ACS Omega 2019, 4, 22214−22227

Table 2. IC_{50} Values of DOX-Loaded Magnetic Nanoparticles (Mag-Alg-PEG-FA/DOX) and Free Dox (DOX)

	MCF-7		MDA-MB 231	
IC_{50} (ppm)	without magnet	with magnet	without magnet	with magnet
Mag-Alg-PEG-FA/DOX	12	4	2.6	1.5
DOX	1.66	1.7	2.7	2.8

with the MDA-MB 231 cells, the IC_{50} values of the DOX-loaded nanoparticles are comparable to or lower than the IC_{50} of free DOX.

After a 24 h incubation of free DOX, DOX-loaded nanoparticles, and blank nanoparticles with the cells, at equivalent DOX concentration (5 μg/mL), the DOX-loaded nanoparticles stimulated significantly higher degree of apoptosis than free DOX in MCF-7 ($p < 0.05$) and in MDA-MB 231 ($p < 0.005$) cell lines (Figure 5). When a magnetic field gradient (0.5 T) was applied, the triggered rate of apoptosis by the DOX-loaded nanoparticles was significantly enhanced in both the MCF-7 ($p < 0.05$) and the MDA-MB 231 ($p < 0.005$) cell lines (Figure 5).

Cellular Uptake. The Mag-Alg-PEG-FA nanoparticles were labeled with rhodamine to investigate their cellular uptake by the MCF-7 and MDA-MB 231 cells. The rhodamine content of the labeled nanoparticles was 3.06% (w/w) (Table 1). The leakage of rhodamine from the nanoparticles was very low (<15%) within a 24 h period (SI Figure S4). In the MCF-7 cells, the uptake of the nanoparticles increased with time from 1 to 4 h ($p < 0.05$) and more significantly to 24 h ($p < 0.005$) (Figure 6A, green column difference). The application of a magnetic field gradient (0.5 T) increased ($p < 0.05$) the uptake of the nanoparticles by the MCF-7 cells at each time period of 1, 4, and 24 h (Figure 6A, green/blue column difference). As for the MDA-MB 231 cells, the uptake of the nanoparticles increased significantly with incubation time (Figure 6B, green column comparison). Under the application of a magnetic field gradient (0.5 T) during nanoparticle−MDA-MB 231 cells incubation, the uptake was significantly ($p < 0.0001$) enhanced at all time periods of 1, 4, and 24 h (Figure 6B, green/blue column comparison at each incubation time). At all times, the uptake of nanoparticles by the MDA-MB 231 cells was significantly higher compared to that by the MCF-7 cells, especially under the influence of a magnetic field gradient (Figure 6C,D).

Fluorescent confocal microscopy was used to visualize the uptake of the rhodamine-labeled Mag-Alg-PEG-FA co-MIONS by the MDA-MB 231 (Figure 7 and SI Figure S7) and MCF-7 cells (SI Figures S5 and S6), with and without the application of a magnetic field gradient (0.5 T). In agreement with the quantitative analysis of cellular uptake (Figure 6), increased internalization was observed in the case of the MDA-MB 231 cells compared to the MCF-7 cells. With the former cells, the magnetic nanoparticles were co-localized with the acidic compartments at early times (1 and 4 h incubation), while at longer incubation periods (24 h), they were mostly co-localized with the nuclei of the cells (Figure 7 and SI Figure S7). In the case of MCF-7 cells, low internalization was observed at early times; specifically, at 1 h, the nanoparticles could barely be noticed, and at 4 h, a low localization with the acidic compartments was revealed. At a relatively long incubation period of 24 h, however, a higher nanoparticle internalization was observed and the nanoparticles were co-localized with the acidic compartments (SI Figures S5 and S6).

Hemolysis Assay. Biocompatibility is a key feature that drug delivery systems should possess for use in biomedical applications. The hemocompatibility of the Mag-Alg-PEG-FA nanoparticles was evaluated here by a hemolysis test, to determine the hemolytic potential of the nanoparticles. In particular, hemolysis is associated with hemoglobin release into the surrounding fluid (blood plasma or normal saline) caused by the disruption (lysis) of the erythrocyte membrane in vivo (general blood circulation) or in vitro (normal saline). Mag-Alg-PEG-FA nanoparticles were evaluated for their hemolytic activity in human red blood cells (RBC, erythrocytes) (Figure 8). The hemolysis at all nanoparticle concentrations tested (up to 2 mg/mL) did not exceed 2% (Figure 8A), indicating the absence of the hemolytic activity of the Mag-Alg-PEG-FA nanoparticles.[17]

DISCUSSION

MIONs have great advantages, mainly because of their enhanced biocompatibility and their superparamagnetic properties. Recent studies by our group have focused on the development of condensed magnetic iron oxide nano-assemblies (co-MIONs) in mild conditions and in aqueous media, where the produced nanosystems exhibit enhanced

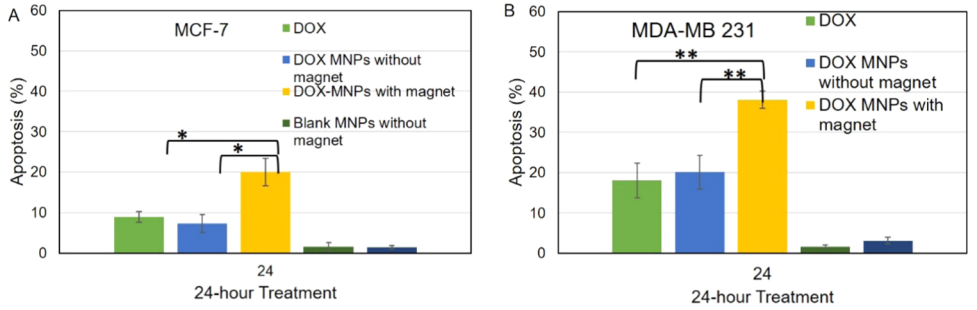

Figure 5. Evaluation of cancer cell apoptosis caused by the DOX-loaded Mag-Alg-PEG-FA nanoparticles. Apoptosis of (A) MCF-7 cells and (B) MDA-MB 231 cells after 24 h of incubation with free DOX (5 μg/mL), DOX-loaded Mag-Alg-PEG-FA nanoparticles (43.48 μg of nanoparticles equivalent to 5 μg/mL DOX), and blank Mag-Alg-PEG-FA nanoparticles (43.48 μg) in the presence (+) and absence (−) of an external magnetic field (permanent magnet field of 0.5 T). Dox: doxorubicin; MNP: magnetic nanoparticles. Asterisks indicate the statistical significance of the difference between results obtained for DOX-loaded nanoparticles and free DOX and DOX-loaded nanoparticles (A) with and (B) without the magnet field (*$p < 0.05$, **$p < 0.005$).

DOI: 10.1021/acsomega.9b03594
ACS Omega 2019, 4, 22214−22227

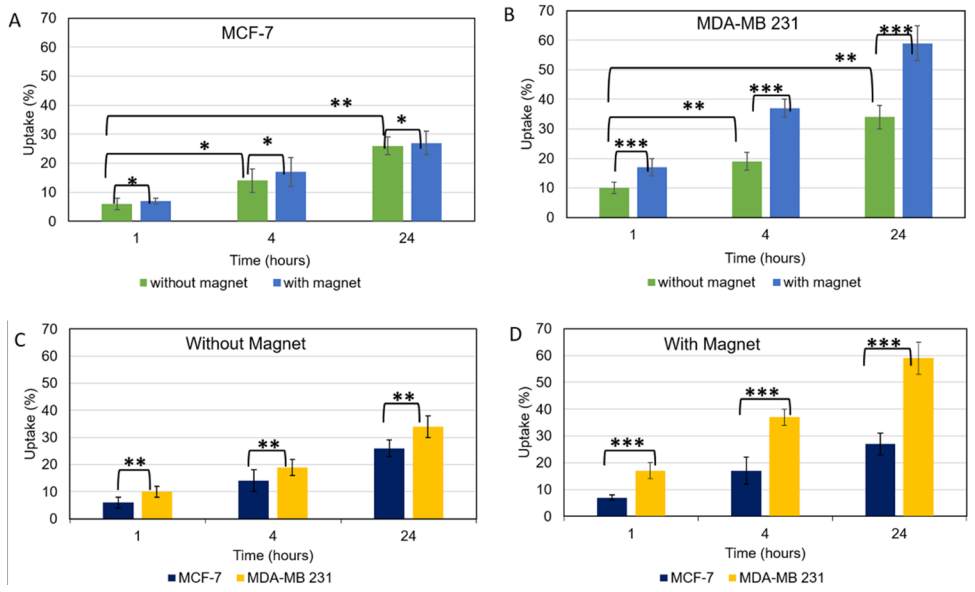

Figure 6. Cellular uptake (%) of rhodamine-labeled Mag-Alg-PEG-FA nanoparticles (43.48 μg of nanoparticles) by (A) MCF-7 and (B) MDA-MB 231 cells after 1, 4, and 24 h of incubation in the presence or absence of an external magnetic field (0.5 T). In (C) and (D), the differences between results at each time period (1, 4, and 24 h) for MCF-7 and MDA-MB 231 cells in the absence and in the presence of a magnetic field (dark blue/yellow column) have been evaluated. *p < 0.05, **p < 0.005, and ***p < 0.0001.

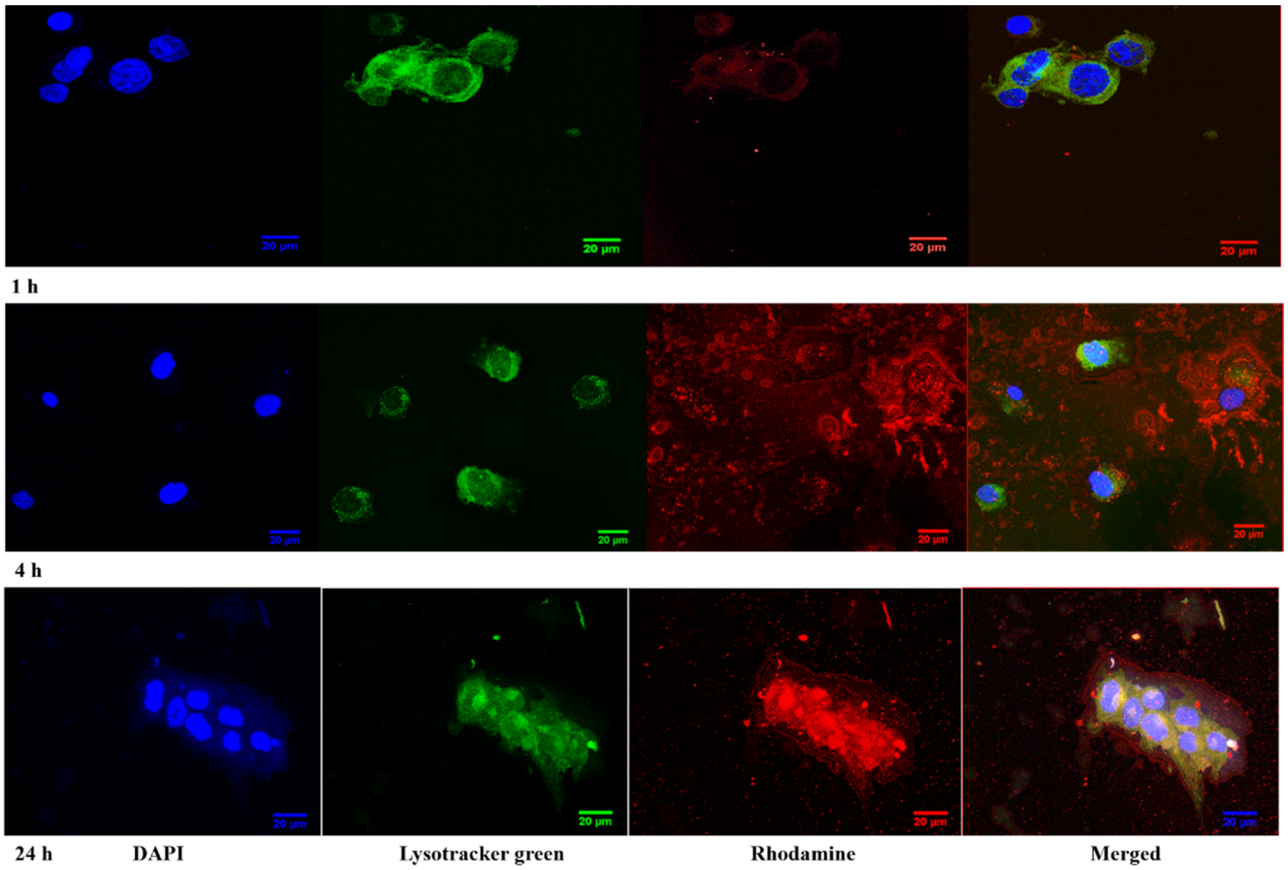

Figure 7. Confocal fluorescence microscopy images of the uptake of rhodamine-labeled Mag-Alg-PEG-FA nanoparticles by the MDA-MB 231 cancer cells at 1, 4, and 24 h under a static magnetic field. From left to right, the panels in each row show fluorescence from 4′,6-diamidino-2-phenylindole (DAPI) (nuclei stained blue), LysoTracker green (staining acidic intracellular compartments), and rhodamine 6G (rhodamine-conjugated nanocarriers, red) and merged images. In merged images, the co-localization of rhodamine with LysoTracker green gives yellow-orange-colored areas and the co-localization of rhodamine with DAPI purple-colored areas.

magnetic properties over other structures or configurations, which is advantageous in magnetic applications and bioimaging.[7,8] Often, in this dense arrangement, the crystallographic planes of magnetic nanocrystals attain the same crystallo-

DOI: 10.1021/acsomega.9b03594
ACS Omega 2019, 4, 22214−22227

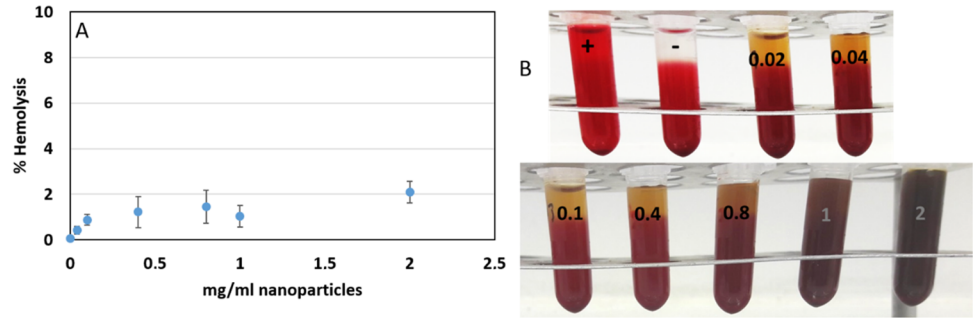

Figure 8. (A) Hemolysis (%) caused by Mag-Alg-PEG-FA nanoparticles after 4 h incubation with red blood cells (RBC) and (B) photos of suspensions of Mag-Alg-PEG-FA nanoparticles with RBCs at varied nanoparticle concentrations. In (B), the symbol (+) indicates the positive control of 100% hemolysis, the symbol (−) indicates the negative control of 0% hemolysis, and the numbers correspond to the nanoparticle concentration in mg/mL.

graphic orientation through their epitaxial aggregation. In this case, the MIONs are in close contact with each other, resulting in an increase in the magnetic field response, due to the increase in the magnetic moment of each colloidal magnetic nanocrystal.

MIONs are susceptible to aggregation due to their increased surface-to-volume-ratio;[18,19] thus, multiple coating methods such as encapsulation,[20,22] micelle formation,[23] coaxial electrospray,[24] microbeads,[25] conjugations,[26−28] and colloidal suspensions[26−28] with biocompatible polymers[20,22−28] or with biopolymers[21,23] have been used for their effective surface modification. Most specifically, the magnetic nanoparticles can be suitably modified with polysaccharides (dextran, alginate, and carboxymethylcellulose) or PEG,[7−10] which will offer them colloidal stability and the ability to be surface-modified. In general, polysaccharides such as alginic acid are biocompatible polymers that can provide free carboxyl groups for attachment (electrostatic or conjugation) of drug molecules as well as for binding of other molecules that add to the particular functionalities of nanoparticles (cell targeting and bioimaging), such as proteins, targeting agents (e.g., folic acid), and fluorescent labels.[6,18−21]

In this study, the alginate co-MIONs were improved by applying a more effective pegylation, using a PEG polymer of 5000 Da in contrast to the PEG polymer of 2000 Da used in previous studies with the alginate co-MIONs,[8] to increase stability in biorelevant media (Figure S3) and by functionalization with folic acid-targeting ligands. In this way, the nanoparticles should gain biological stability to maintain their structural integrity, preventing them from aggregation when found in the general circulation of blood after intravenous administration, and molecular targeting properties that will lead to selective and efficient endocytosis of the nanoparticles (and hence of the drug they carry) to the cancer cells.

The here-developed Mag-Alg-PEG-FA magnetic nanoparticles had an average size (hydrodynamic diameter) of around 95 nm (Table 1), which is appropriate for their accumulation in the tumor tissue upon intravenous administration, taking advantage of the EPR phenomenon[11] and their guided assembly by an external magnetic field applied at the tumor site. The Mag-Alg-PEG-FA nanoparticles did not aggregate, expressing good stability in biorelevant media (such as blood plasma, Figure 2), suggesting that they will retain their optimum size characteristics in vivo in blood circulation, to exhibit the desired biodistribution properties (accumulation in tumors due to the EPR effect and the application of external magnetic fields at the tumor site). The enhanced stability of the Mag-Alg-PEG-FA nanoparticles observed here can be attributed to the presence of poly(ethylene glycol) (PEG 5000 Da molecular weight), which would reduce the interactions between the nanoparticles and biorelevant media constituents, such as proteins. The binding of proteins (opsonins) on the nanoparticle surface in vivo (opsonization) leads to rapid uptake by the reticuloendothelial system and removal of nanoparticles from general circulation.[29] Rapid removal of nanoparticles from the blood does not allow them to accumulate at their site of action (tumor area).

Effective control of drug release (doxorubicin) by Mag-Alg-PEG-FA nanoparticles was achieved, since DOX release was very low at blood pH (PBS of pH 7.4), while increased release was observed at the acidic pH (PBS of pH 6) and in biorelevant media (blood plasma and RPMI-1640 cell culture medium) (Figure 3A). The acidic pH conditions offer a proton-rich environment that leads to the protonation of the carboxylic groups of alginate, reducing the electrostatic attraction of the positively charged DOX molecules to alginate and facilitating DOX leakage from the nanoparticles.[18,19] Since tumor tissues constitute an acidic environment and the intracellular compartments of cancer cells (endosomes and lysosomes) provide even lower pH than the extracellular environment (around 5.0−5.5),[30] and providing DOX will have a similar release behavior from the nanoparticles in vivo, the pH-responsive release behavior of DOX from Mag-Alg-PEG-FA nanoparticles is potentially important with regard to the in vivo anticancer efficacy of DOX-loaded Mag-Alg-PEG-FA nanoparticles. Enhanced DOX release was observed in biorelevant media compared to the buffer with pH 7.4 (Figure 3); however, even in these media, DOX release was efficiently sustained, with only around 60% release in 48 h. Provided that similar DOX release rates will exist in vivo, this would give enough time window to the nanoparticles to reach the tumor site before any significant drug leakage occurs. The enhanced DOX release from the nanoparticles in the biorelevant media compared to the aqueous buffer is possibly due to the antagonistic effect of the proteins (in plasma) and growth factors (in RPMI with FBS 10% v/v) with DOX for the carboxylic sites of the carrier. Since human blood plasma is mainly composed of serum albumin (55%), globulins (38%), and fibrinogen (7%), it is a highly heterogeneous medium of amphiphilic and hydrophilic proteins and one cannot exclude that the antagonistic effect of plasma proteins on DOX binding on the nanoparticles may also involve hydrogen bonding and hydrophobic interactions, besides electrostatic interac-

DOI: 10.1021/acsomega.9b03594
ACS Omega 2019, 4, 22214−22227

tions.[31−33] Magnetically triggered DOX release was observed from the nanoparticles under the influence of an AC magnetic field[33,34] (Figure 3B). The release experiment was conducted at low Mag-Alg-PEG-FA nanoparticle concentration (<0.1% w/w in Fe_2O_3); thus, no macroscopic temperature rise in drug release medium was observed. Therefore, the enhanced magnetic drug release under the applied AC magnetic field was probably the outcome of the heat released from the MION assemblies resulting in the local heating of the polymeric shell of the nanoparticles.[33,35,36] Another contributing factor to the enhanced drug diffusion could be the mechanical rotation of the MION assemblies under the influence of the AC magnetic field.[33,34] The effect of the magnetic field on DOX percentage release appeared to be independent of the timing (onset time) of the magnetic field application (Figure 3B), providing flexibility and simplifying, thus, the magnetic control of drug release from the co-MIONS in the in vivo situation.

The DOX-loaded Mag-Alg-PEG-FA nanoparticles exhibited dose-dependent cytotoxicity, lower than or similar to that of free DOX, against the MCF-7 cells, which do not express the folate receptor (FL1R), while higher cytotoxicity than that of free DOX was observed against the MDA-MB 231 cells, which express the FL1R receptor (Figure 4). The enhanced cytotoxicity of the loaded nanoparticles versus free DOX against the MDA-MA-231 cells (Figure 4C,D) is probably associated with the increased rate of apoptosis induced by the DOX-loaded nanoparticles in these cells (Figure 5). The observed apoptosis data are in agreement with the DOX effect on apoptosis and oxidative stress against these breast cancer cell lines.[37] The DOX-loaded nanoparticles exhibited increased cytotoxicity with lower IC_{50} values (Table 2) and induced the increased rate of apoptosis against the MCF-7 and MDA-MB 231 cancer cells, in the presence of a static magnetic field (Figures 4B,D and 5). This effect is probably related to the increased rate of nanoparticle internalization by the cells (internalization is expressed as the percentage uptake vs incubation time, Figure 6) and thereby to the higher rate of uptake of the drug entrapped in the nanoparticles, in the presence of the magnetic field. The uptake of the nanoparticles by the MCF-7 cells not expressing the folate receptor indicates that the FR-receptor-mediated endocytosis (RME) was not the only endocytic pathway of the magnetic nanoparticles uptake, as was also reported recently by Allard-Vannier et al. for folic acid-functionalized SPIONs.[32] The uptake of the Mag-Alg-PEG-FA nanoparticles by the cancer cells was visualized with confocal microscopy (Figures 7 and S5−S7). In the absence of a magnetic field, the nanoparticles are co-localized with the lysosomes in both cell lines at prolonged time of incubation (24 h, Supporting Information Figures S6 and S7). In the case of the MCF-7 cells, which do not express the FA receptor, receptor-mediated endocytosis (RME) cannot be responsible for nanoparticle internalization. As was reported recently by Allard-Vannier et al.,[32] RME is not the only possible endocytic pathway for superparamagnetic nanoparticles (such as SPIONs and MIONs), proposing a clathrin-dependent endocytosis (CDE) in breast cancer cells not expressing the FA receptor, such as the MDA-MB 435 cells. CDE is characterized by the involvement of clathrin (a triskelion-shaped protein scaffold), which polymerizes around the cytoplasm, acting as a reinforcing matrix that facilitates the internalization and recycling of a variety of receptors such as tyrosine kinase receptors, uptake of low-density lipoprotein, and recycling of iron-bound transferrin. Probably, the superparamagnetic iron nanoparticles are recognized by the clathrin polymer network, leading to their internalization.[38]

The presence of a static magnetic field highly accelerated nanoparticle uptake by MDA-MB 231 cells even at early times (4 h incubation, Figure 7), where a granular distribution of the nanoparticles in the cytoplasm was observed and accumulation even in the nucleus was observed at 24 h. The presence of the magnetic field did not increase the nanoparticle uptake by MCF-7 cells at early times (1 and 4 h); however, an overall increase of co-localization with the cytoplasm and the nucleus was observed at a long incubation period (24 h, Supporting Information Figure S5). The enhancement of nanoparticle uptake by the cancer cells in the presence of the external magnetic field suggests the importance that magnetic targeting may have in increasing the anticancer efficacy of nano-formulations based on co-MIONs.

The Mag-Alg-PEG-FA nanoparticles exhibited no hemolytic activity (Figure 8), and this result, together with the absence of cytotoxicity of the nanoparticles, is indicative of the biocompatibility of these nanoparticles. It is recognized, however, that more studies are required to establish the biocompatibility and safety of the Mag-Alg-PEG-FA nanoparticles for drug delivery applications.

CONCLUSIONS

In this study, pegylated co-MIONs, functionalized with FA and loaded with DOX, were synthesized. These magnetic nanoparticles exhibited controlled DOX release, even in biorelevant media (human blood plasma and RPMI-1640 cell culture medium), which could be accelerated at an acidic pH or in response to an alternating magnetic field. The FA-functionalized co-MIONs caused increased apoptosis and cytotoxicity against the MDA-MB-231 cell line, expressing the folate receptor, compared to the MCF-7 cell line, not expressing the folate receptor. Also, the nanoparticles exhibited increased uptake by and increased cytotoxicity against the MDA-MB 231 cells under the influence of a static magnetic field. These results suggest the potential of the folate-functionalized, pegylated co-MIONS for a more efficacious DOX delivery to cancer cells of solid tumors.

EXPERIMENTAL SECTION

Materials. Iron(II) sulfate heptahydrate ($FeSO_4{\cdot}7H_2O$, assay > 99%, Chem Lab NV, Zedelgem, Belgium), sodium alginate (Na-alginate, Sigma-Aldrich; the viscosity of 2% solution at 25 °C: ∼250 cps), HCl (37%, Carlo Erba, Barcelona), ammonium hydroxide (NH_4OH, 30% for analysis, Carlo Erba) were used for the synthesis of the nanoparticles. OH-PEG-NH_2 (average molecular mass 5000 Da, RAPP Polymers) was used for the PEGylation reaction. Coupling reagents used were *N*-ethyl-*N*′-(3-dimethyl aminopropyl) carbodiimide hydrochloride (EDC HCl, assay > 98%, 191.7 g/mol), *N*-hydroxysulfosuccinimide (s-NHS, assay > 98%, 217.14 g/mol), *N*,*N*-diisopropylethylamine (DIPEA, Merck), hydroxybenzotriazole (HOBt, CBL Patras), and folic acid (FA, assay > 98%, 441.4 g/mol). The fluorescent agent for the nanoparticles *N*-(2-aminoethyl)rhodamine 6G-amide bis-(trifluoroacetate) (rhodamine 6G, assay ≥ 95.0%) was purchased from Sigma-Aldrich, and for cellular studies, LysoTracker Green (Invitrogen, CA) and 4′,6-diamidino-2-phenylindole dihydrochloride (DAPI assay ≥98%, Sigma-Aldrich) were used. DOX hydrochloride was from Sigma-

DOI: 10.1021/acsomega.9b03594
ACS Omega 2019, 4, 22214−22227

Aldrich. All other chemicals and solvents were of analytical grade. Human blood plasma was obtained from the University Hospital of Patras, Greece. In the experiments, ultrapure 3D-H_2O from an ELGA MEDICA apparatus was used.

Synthesis and Characterization of Mag-Alg-PEG-FA Nanoparticles. *Synthesis of Mag-Alg Nanoparticles.* The alginate-coated condensed magnetic nanoparticles (co-MIONs) were synthesized according to our previously described protocols of the alkaline precipitation method.[7−10] In brief, $FeSO_4 \cdot 7H_2O$, used as a precursor, predissolved in 3D-H_2O (20 mL with 60 μL of 37% HCl), was added in a sodium alginate solution in water (300 mg in 60 mL of 3D-H_2O with 4 mL of NH_4OH). The reaction was performed at 50 °C under magnetic stirring for 80 min. The product (Mag-Alg) was centrifuged for purification (14 000 rpm for 35 min) where the supernatant containing byproducts was discarded, and the precipitate was fractionated (4000 rpm for 20 min) where the supernatant containing the final product was kept. The purification/fractionation process was repeated in triplicate.

Synthesis of Mag-Alg-PEG Nanoparticles. The pegylation process of the Mag-Alg condensed nanoparticles was based on Sarigiannis et al.[8] report with slight modifications. The reaction was performed in dimethylformamide (DMF); thus, the nanoparticle dispersion solvent was changed from 3D-H_2O to DMF. Thus, dialysis was required for 48 h in D-H_2O (pH 4.3), to protonate alginate carboxyl groups. The exchange from the aqueous to organic solvent was performed with repeated centrifugation (15 000 rpm for 20 min), twice in D-H_2O followed by centrifugation (15 000 rpm for 20 min) twice in DMF. After each centrifugation cycle, the supernatant including the byproducts was discarded and the precipitate with the magnetic nanoparticles was resuspended in the desired solvent. After the final centrifugation step, DIPEA (10 μL/mL) was added in the Mag-Alg nanoparticle dispersion in DMF. For the pegylation, OH-PEG-NH_2 was added in Mag-Alg dispersion (of 3 mg/mL in DMF) at a molar ratio of $-COOH/-NH_2$ = 1:1.6, under bath sonication for 15 min. For the activation of carboxyl groups of Mag-Alg, EDC/HOBt predissolved in DMF was added at a molar ratio of −COOH:EDC/HOBt = 1:5 (in mole), producing a final EDC concentration of 10 mM (the final volume of reaction solution was 1 mL). The mixture was left to react for 10 min under bath sonication and was then incubated in a gently agitated water bath at ambient temperature (25 °C) for 24 h in the dark. The final mixture was centrifuged (15 000 rpm for 20 min) in DMF, and the precipitate containing the final product (Mag-Alg-PEG) was redispersed in 3D-H_2O (the final volume of 1 mL). Purification of the final product was performed by centrifugation (15 000 rpm for 20 min) in 3D-H_2O repeated in triplicate.

Synthesis of Mag-Alg-PEG-FA Nanoparticles. To prepare folic acid-functionalized Mag-Alg-PEG nanoparticles, carbodiimide chemistry was used to link the carboxyl groups (−COOH) of FA with the hydroxylic groups (−OH) of PEG (ester bonding). An aqueous solution of Mag-Alg-PEG nanoparticles was used (67 μL from stock of 5 mg/mL in the final volume of 2 mL).[12,13] The concentration used for the conjugation was Mag-Alg-PEG/FA = 1:1.3 (in mg) and the molar ratio for the activation was FA:EDC/s-NHS = 1:5, producing a final concentration of EDC = 2.11 mM (the final volume of reaction solution was 1 mL). For the conjugation reaction, in an aqueous solution of FA (the final volume of 200 μL), EDC/s-NHS predissolved in cold 3D-H_2O (20 μL volume) was added dropwise within 5 min, under bath sonication to activate carboxyl groups (−COOH) of FA. Then, activated FA was added dropwise in Mag-Alg-PEG aqueous solution (the final volume of 1 mL) within 15 min, under bath sonication. The reaction mixture was bath-sonicated for 1 h, after which it was transferred to a gently agitated water bath at ambient temperature (25 °C) for 24 h in the dark. The final product (Mag-Alg-PEG-FA nanoparticles) was transferred to a cuvette holder, and magnetic separation/purification was used by adjusting a cylindrical neodymium magnet (Nd-Fe-B of 0.5 T, dimensions: 20 mm × 10 mm) along with the cuvette for 24 h, at ambient temperature (25 °C), in a calm environment, in the dark. The pellet formed after magnetic purification containing the final product (Mag-Alg-PEG-FA nanoparticles, 200 μg/mL final product) was assayed spectrophotometrically at 365 nm, and the data were corrected for the absorbance of plain (without FA) nanoparticles at the same wavelength. The quantification was based on an FA calibration curve (R^2 = 0.99998) in NaOH (0.01 M).

Characterization of Mag-Alg-PEG-FA Nanoparticles. The morphology of the synthesized nanoparticles was investigated by transmission electron microscopy (TEM), wherein samples were prepared by casting a droplet of a dilute aqueous suspension of nanoparticles (0.01% w/v in Fe_2O_3) on copper grids coated by a Formvar carbon film. Images were obtained by a JEOL, JEM-2100 instrument operating at 200 kV. The determination of the hydrodynamic diameter (average diameter [D_h] and polydispersity index [PDI]) of nanoparticles dispersed in 3D-H_2O was performed using a ZetaSizer Nano series Nano-ZS (Malvern Instruments Ltd., Malvern, U.K.) equipped with a He−Ne laser beam at a wavelength of 633 nm and a fixed backscattering angle of 173°. The ζ-potential of the nanoparticles was assessed using the same instrument as the average of 100 runs with the phase analysis light scattering mode, after equilibration at 25 °C. The composition of the nanoparticles was investigated by thermogravimetric analysis (TGA) on a TA Instrument Q500 series thermogravimetric analyzer at a heating rate of 10 °C/min from room temperature to 700 °C in a nitrogen (N_2) atmosphere. The successful functionalization of MIONs after each conjugation step was probed by ATR spectroscopy. The ATR spectra were recorded in an FTS 3000 Excalibur Series Digilab spectrometer with an ATR adaptor of PIKE MIRacle.

The colloidal stability of the magnetic nanoparticles was assessed in Roswell Park Memorial Institute (RPMI) 1640 cell medium and human blood plasma (50% v/v in water). The nanoparticle samples (100 μL of 3 mg/mL concentration and 0.51% w/v Fe_2O_3) were dispersed in RPMI-1640 cell culture medium and in human blood plasma (the final volume of 1 mL) and incubated for 1, 5, and 24 at 37 °C under gentle agitation. After the desired time periods, the samples were magnetically separated. Then, the precipitated nanoparticles were redispersed in 3D-H_2O, and their size (hydrodynamic diameter) and ζ-potential were measured by dynamic light scattering (DLS), as described in the above paragraph.

Labeling of Mag-Alg-PEG-FA Nanoparticles. The Mag-Alg-PEG-FA nanoparticles were labeled with *N*-(2-aminoethyl)rhodamine 6G-amide bis(trifluoroacetate) (rhodamine, Rh) fluorescent dye by applying carbodiimide chemistry to link the amine groups ($-NH_2$) of rhodamine with the carboxylic groups (−COOH) of alginate (amide bonding).[12,13] An aqueous solution of Mag-Alg-PEG-FA

DOI: 10.1021/acsomega.9b03594
ACS Omega 2019, 4, 22214−22227

nanoparticles was used (67 μL from stock of 5 mg/mL in the final volume of 2 mL). The molar ratios for the activation were −COOH(of Alg.)/−NH_2(of Rh.) = 1:4 and −COOH(of Alg.):EDC/s-NHS = 1:5, producing a final concentration of EDC of 10 mM (the final volume of reaction solution was 1 mL). A similar procedure described above for FA conjugation to PEG was followed. In brief, in a Mag-Alg-PEG-FA aqueous solution, rhodamine (100 μL from a stock solution of 1 mg/mL) was added under bath sonication for 15 min. Then, predissolved EDC/s-NHS in cold 3D-H_2O (20 μL) was added dropwise within 5 min, under bath sonication to activate carboxyl groups (−COOH) of alginate. The reaction mixture was bath-sonicated for 1 h, after which it was transferred to a gently agitated water bath at ambient temperature (25 °C) for 24 h in the dark. The final product (Mag-Alg-PEG-FA-Rh nanoparticles) was transferred to a cuvette holder, and magnetic purification was used by adjusting a cylindrical neodymium magnet (Nd-Fe-B of 0.5 T, dimensions: 20 mm × 10 mm) along with the cuvette for 24 h, at ambient temperature (25 °C), in a calm environment, in the dark. The pellet formed after magnetic separation contained the final product (Mag-Alg-PEG-FA nanoparticles). The amount of rhodamine that had not been conjugated on the nanoparticles was measured spectrophotometrically in the supernatant (3D-H_2O) after the magnetic separation. Then, by subtraction from the total amount of rhodamine initially applied, the fraction of rhodamine conjugated to the nanoparticles was calculated. The rhodamine absorbance in the supernatants was measured at 529 nm, and the quantification was based on a calibration curve (R^2 = 0.9978).

Drug Loading. In dispersions of Mag-Alg-PEG-FA nanoparticles (200 μg in 0.5 mL of water), DOX aqueous solution of 50, 100, 150, and 200 μL were added (from a DOX stock solution of 1 mg/mL), and the final volume of each experiment was adjusted to 1 mL.[10] The mixtures were then incubated in a gently agitated water bath (25 °C) for 24 h in the dark. Subsequently, the DOX-loaded nanoparticles were magnetically separated by adjusting a cylindrical neodymium magnet (Nd-Fe-B of 0.5 T, dimensions: 20 mm × 10 mm) along with the cuvette for 24 h at ambient temperature (25 °C) in the dark. The precipitate containing the DOX-loaded nanoparticles was resuspended in the initial volume of 3D-H_2O (1 mL). The supernatant, containing the nonentrapped DOX fraction, was freeze-dried and reconstituted in 3D-H_2O (the final volume of 1 mL) and filtered through a Millipore filter of 0.45 μm diameter. DOX in the filtered samples was quantified spectrophotometrically by a Shimadzu UV-1800 spectrophotometer. The absorbance of the sample was measured at 480 nm, and the DOX concentration was calculated using a calibration curve (R^2 = 0.9998). The limit of quantification was 5 μg/mL, and the linear part of the standard curve used for the DOX assay was from 5 to 50 μg/mL. The fraction of DOX entrapped in the magnetic nanoparticles was estimated by subtracting the nonconjugated quantity of DOX from the total amount (feed) of DOX initially added in the nanoparticles.

The loading capacity and entrapment efficiency of DOX in Mag-Alg-PEG-FA magnetic nanoparticles were calculated from the following equations

$$\mathrm{LC\%} = \frac{W_{\mathrm{DOX}}}{W_{\mathrm{nps}} + W_{\mathrm{DOX}}} \times 100 \quad (1)$$

where W_{DOX} and W_{nps} were the amount of attached drug and the amount of Mag-Alg-PEG-FA nanoparticles, respectively.

In Vitro Drug Release. DOX release from the Mag-Alg-PEG-FA magnetic nanoparticles was determined in PBS of varied pH values (pH = 6.0 and 7.4) at 37 °C. The ionic strength of the phosphate buffer was 154 mM, similar to the 149.5 mM of human blood plasma.[12,13] Thus, DOX-loaded Mag-Alg-PEG-FA nanoparticles (1 mL including 23 μg of DOX and 200 μg of nanoparticles) were enclosed in dialysis sacs (molecular weight cutoff = 12 kDa) and incubated to 10 mL of phosphate buffer at 37 °C under gentle agitation in a water bath in the dark. At predetermined time intervals (30 min and 1, 2, 4, 6, 24, and 48 h), the entire release medium was removed and replaced by fresh PBS prewarmed at 37 °C. The release medium containing DOX was assayed by UV−vis spectroscopy at 480 nm. The amount of released DOX, for each release medium (pH = 7.4 and 6), was calculated based on separate calibration curves (for pH = 7.4: R^2 = 0.9994 and for pH = 6: R^2 = 0.9981) by dissolving known concentrations of DOX in the desired phosphate buffer. The limit of quantification for pH = 7.4 was 0.1 μg/mL and for pH = 6 was 0.05 μg/mL. The linear part of the standard curve used for DOX assay for pH = 7.4 was from 0.1 to 50 μg/mL and for pH = 6 was from 0.05 to 50 μg/mL.

DOX release from the Mag-Alg-PEG-FA nanoparticles was also determined under the influence of an alternating magnetic field (f = 110.6 kHz, B = 25 mT, I = 12.2 A, and V = 28.3 V), following the process described above. The magnetic field was applied for 15 min during the second and fourth hours of release at pH 6.0, using magnetic fluid hyperthermia (MFH) by MagneTherm device from NanoTherics, thermostated at 37 °C.

The release of DOX from the Mag-Alg-PEG-FA nanoparticles in RPMI-1640 cell medium[14] (with 10% v/v FBS) and human blood plasma[15] (10% v/v in PBS) was also determined as described above. In brief, DOX-loaded Mag-Alg-PEG-FA nanoparticles (23 μg of DOX and 200 μg of nanoparticles) were suspended in RPMI-1640 (10% FBS) or human blood plasma (10% v/v) (the total medium volume of 1 mL) and enclosed in dialysis sacs (molecular weight cutoff = 12 kDa). The sacs were then incubated in the respective (RPMI or plasma) biorelevant medium (the total outer volume of 5 mL) at 37 °C under gentle agitation in a water bath in the dark. At predetermined time intervals (30 min and 1, 2, 4, 6, and 24 h), the entire release medium was removed, transferred to centrifugation tubes, and replaced by fresh medium prewarmed at 37 °C. At each time point, the tubes were centrifuged at 15 000 rpm for 10 min and the supernatant, containing the released DOX, was kept. The precipitate (contained precipitated proteins) was resuspended in DD water (1 mL) to be centrifuged again, so as to fully extract the released DOX. Dimethyl sulfoxide (DMSO) was used to precipitate the remaining plasma and RPMI proteins of the supernatants. Thus, after both centrifugations, the supernatants (the total volume of 6 mL) were mixed with DMSO at a ratio of 1:1 v/v and centrifuged at 15 000 rpm for 10 min. After this final centrifugation, proteins in the precipitate were discarded and the supernatant containing only the released DOX (more than 90%) was assayed in a UV−vis spectrophotometer at 480 nm. The complete process was repeated twice. For the calculation of the amount of released DOX, standard curves of known concentrations of the drug were prepared, following the above described process, in each biorelevant medium (RPMI-

DOI: 10.1021/acsomega.9b03594
ACS Omega 2019, 4, 22214−22227

1640: R^2 = 0.9987 and human blood plasma: R^2 = 0.9977). The limit of quantification for DOX in RPMI-1640 was 0.1 μg/mL and in human blood plasma was 0.05 μg/mL. The linear part of the standard curve used for DOX assay in RPMI-1640 was from 0.1 to 50 μg/mL and in human blood plasma was from 0.05 to 50 μg/mL.

In Vitro Cellular Studies. *Cell Lines.* The human breast adenocarcinoma cancer cell lines MDA-MB 231 (expressing the FA receptor FL1R) and MCF-7 (not expressing the FA receptor) obtained from the European Collection of Cell Cultures-Health Protective Agency (ECACC-HPA) were cultured in 75 cm^2 flasks (5520200, Orange Scientific) in RPMI-1640 medium supplemented with 10% (v/v) fetal bovine serum (FBS) and a mixture of antibiotic agents (1.1% v/v penicillin/streptomycin and 0.15% v/v amphotericin). Cultures were maintained at 37 °C in a humidified (100%) atmosphere with 95% (v/v) air and 5% (v/v) CO_2. The culture medium was changed every 48 h, and cells were harvested with 0.25% (w/v) trypsin in PBS.

Viability. DOX-loaded Mag-Alg-PEG-FA nanoparticles were assayed for the in vitro anticancer activity (cytotoxicity) by the MTT method (3-[4,5-dimethylthiazol-2-yl]-2,5-diphenyl tetrazolium bromide), as described.[39] MDA-MB 231 and MCF-7 cells were seeded into 24-well plates at a density 1×10^4 cells/well and allowed to attach and proliferate as a monolayer under standard conditions for 24 h. Then, the supernatant in each well was completely removed and substituted with fresh medium (500 μL of RPMI) consisting of different concentrations of free DOX (0.05, 0.5, 5, and 10 μg/mL) or DOX-loaded magnetic nanoparticles (0.43, 4.34, 43.48, and 86.9 μg/mL), producing equivalent drug quantities to those of free DOX. The cytotoxicity of blank (without DOX) magnetic nanoparticles was also evaluated, at concentrations consistent to the carrier concentrations of DOX-loaded nanoparticles. The assayed concentrations of DOX were selected through a preliminary evaluation of free DOX in the range 0.01−15 μg/mL, to determine the IC_{50} of the drug on MCF-7 and MDA-MB 231 cells. Following a 24 h incubation at 37 °C, the supernatant was completely removed, the cells were washed twice with PBS, and in each well 100 μL of fresh RPMI medium was added supplemented with 10 μL MTT solution (from stock solution of 12 mM in PBS [5 mg of MTT/1 mL of PBS]). The plates were incubated at 37 °C for 4 h, and then, the medium was completely removed. Next, 150 μL of DMSO was added in each well followed by incubation at 37 °C for 15 min, under gentle agitation, to dissolve the formazan crystals. The absorbance of the plates was measured using an MPR-700 Plate Reader, Biotech Engineering Management Co. Ltd (U.K.). Absorbance was measured at 492 nm, and a second wavelength at 590 nm was measured to subtract the background "noise". Cytotoxicity was expressed as reduction in cell viability (%). The experiments were performed in triplicates. The IC_{50} values of DOX and DOX-loaded magnetic nanoparticles were calculated from the percentage cell viability versus concentration data by fitting the dose−effect curves according to a four-parameter logistic model with OriginPro 8 software (Origin Lab Corp, Northampton, MA).[12,13]

Apoptosis. In cells, the loss of cellular membrane integrity causes phosphatidylserine externalization, which is associated with apoptotic or necrotic processes and marks the later stages of cell death.[12,13] Cells are considered to be in late apoptosis or already dead if they are both Annexin V and PI positive; cells in early apoptosis are Annexin V positive and PI negative, while viable cells are both Annexin V and PI negative. In this study, Annexin V protein (FITC-Annexin V, BD Pharmingen) was used as a marker of apoptosis to detect the externalization of phosphatidylserine, as described.[13]

MCF-7 and MDA-MB 231 cells were plated into 24-well plates at a density of 1×10^4 cells/well and allowed to attach and proliferate under standard conditions as a monolayer for 24 h. Then, the supernatant in each well was removed completely and replaced with fresh RPMI medium supplemented with blank (without DOX) nanoparticles (43.48 μg/mL), DOX-loaded Mag-Alg-PEG-FA nanoparticles (43.48 μg/mL corresponding to the DOX concentration of 5 μg/mL), and DOX (5 μg/mL). After a 24 h incubation, the supernatant was removed and the cells were washed twice with PBS and detached by trypsinization (0.25% w/v trypsin). Then, the cells placed in FACS tubes were centrifuged (1600 rpm for 5 min) and the pellet was washed and resuspended in 1 mL of 1X Annexin V binding buffer. The cells were again centrifuged (1600 rpm for 5 min), and the pellet was resuspended in 100 μL of 1X Annexin V binding buffer and incubated with 5 μL of FITC-Annexin V in the dark for 15 min at room temperature. After that, the cells were washed with and resuspended in 0.5 mL of Annexin V binding buffer. Cell fluorescence due to Annexin V (% cell apoptosis) was determined by flow cytometry (excitation λ = 495 nm, emission λ = 519 nm), in a FACS Calibur, Coulter Epics XLMCL apparatus. The background fluorescence of unlabeled cells was determined and used as a negative control. Data analysis was performed with the WinMDI cytometry analysis software.

Cellular Uptake. The uptake of rhodamine-labeled Mag-Alg-PEG-FA nanoparticles by MCF-7 and MDA-MB-231 cells, following 1, 6, and 24 h incubation, was evaluated by flow cytometry. Cells seeded in 24-well plates at a density of 1×10^4 cells/well were allowed to grow and proliferate as a monolayer in standard conditions for 24 h. The supernatant was then removed and replaced with fresh medium supplemented with rhodamine-labeled nanoparticles at a concentration of 43.48 μg/mL and incubated for 1, 6, and 24 h. Then, the supernatant was removed and the cells were washed twice with PBS and harvested by trypsinization (0.25% w/v trypsin). Rhodamine fluorescence was measured using FACS (excitation 550 nm, emission 573 nm), in a FACS Calibur, Coulter Epics XLMCL apparatus. The background fluorescence of unlabeled cells was determined and used as a negative control. Data analysis was performed with the WinMDI cytometry analysis software.

The uptake of the rhodamine-labeled magnetic nanoparticles was also measured under the influence of an external static magnetic field using a Nd-Fe-B magnet (0.5 T, with 10 mm diameter and 3 mm height) placed in contact with the outer surface of the cell well plates.

The uptake of the rhodamine-labeled Mag-Alg-PEG-FA nanoparticles by the MCF-7 and MDA-MB-231 cells was visualized by confocal laser microscopy.[13] The cells at a density of 1×10^4 cells/well were plated in 24-well plates and grown on sterilized cover slips (Borosilicate Glass, VWR) placed in each well, under standard conditions described above. After a 24 h incubation, the supernatant in each well was replaced with fresh medium containing the rhodamine-labeled nanoparticles at a concentration of 43.48 μg/mL and incubated for 1, 6, and 24 h. Then, the cells were washed thrice with PBS and stained with a sufficient quantity of 50 nM Lysotracker Green (green fluorescent dye staining the acidic compartments in alive cells)

DOI: 10.1021/acsomega.9b03594
ACS Omega 2019, 4, 22214−22227

for 15 min at 37 °C. Then, the cells were washed thrice with PBS and a sufficient quantity of 300 nM DAPI stain solution (blue fluorescent dye staining nucleic acids) was added. After 10 min incubation at 37 °C, the cells were washed thrice with PBS, drained, and mounted with Mowiol 4-88. The obtained test samples were observed on a Leica SP5 confocal microscope (Germany) equipped with appropriate filters for DAPI (excitation 359 nm, emission 457 nm), rhodamine (excitation 550 nm, emission 573 nm), and Lysotracker Green (excitation 504 nm, emission 511 nm).[13]

Hemolysis Assay. The hemocompatibility of Mag-Alg-PEG-FA nanoparticles was evaluated by a hemolysis assay.[17] In brief, blood samples from healthy donors (obtained from the University Hospital of Patras, Greece) were collected in heparin tubes and centrifuged at 4000 rpm for 10 min for plasma separation. Then, the erythrocytes (red blood cells, RBCs) were washed thrice with normal saline and a ratio of 1:20 pure RBCs was prepared (from the initial volume of 0.5 mL blood in a final volume of 2 mL in normal saline). Then, a suspension of magnetic nanoparticles was prepared in PBS by serial dilution from 0.200 to 0.02 mg/mL. Equal quantities of RBC suspension (0.5 mL) and nanoparticle suspension (0.5 mL) were mixed with a rotator shaker and incubated for 4 h at 37 °C. Then, the tubes were centrifuged (4000 rpm for 10 min) and the supernatant containing the hemoglobin was transferred to 96-well plates and the absorbance of the plates was measured at 570 nm using an MPR-700 Plate Reader, Biotech Engineering Management Co. Ltd (U.K.). The positive control (100% hemolysis) was prepared by suspending RBCs in double-distilled water and the negative control (0% hemolysis) by suspending RBCs in PBS. The test was repeated thrice. The percentage of hemolysis was calculated from the following equations

$$\text{hemolysis}\% = \frac{A_{\text{nps}} - A_{\text{negative}}}{A_{\text{positive}} - A_{\text{negative}}} \times 100 \quad (2)$$

where A_{nps}, A_{negative}, and A_{positive} were the absorbance of hemoglobin contained in the supernatant of the magnetic nanoparticles, the absorbance of the negative control, and the absorbance of the positive control, respectively.

Statistical Analysis. Appropriate statistical methods (Student's *t*-test and one-way analysis of variance for comparison of means) were applied for the statistical analysis of experimental data using the IBM SPSS Statistics 25 software.

■ ASSOCIATED CONTENT

Supporting Information

The Supporting Information is available free of charge at https://pubs.acs.org/doi/10.1021/acsomega.9b03594.

Detailed physicochemical characteristics of magnetic nanoparticles; ATR spectra of magnetic nanoparticles and detailed characterization; colloidal stability results of Mag-Alg-PEG (5 kDa)-FA nanoparticles in comparison with Mag-Alg-PEG (2 kDa); rhodamine release from Mag-Alg-PEG-FA magnetic nanoparticles; and confocal fluorescence microscopy images of the uptake of rhodamine-labeled Mag-Alg-PEG-FA nanoparticles by MCF-7 cancer cells with and without a magnetic field and by MDA-MB-231 without a magnetic field (PDF)

■ AUTHOR INFORMATION

Corresponding Author

*PhD Laboratory of Pharmaceutical Technology, Department of Pharmacy, University of Patras, GR. 26504, Patras, Greece. Tel. 6974987290, 0030 2610962318. Email: angelopoulou@upatras.gr.

ORCID

Athina Angelopoulou: 0000-0001-7277-1590

Funding

This research has been co-financed by the Operational Program "Human Resources Development, Education and Lifelong Learning" and the European Union (European Social Fund) and Greek national funds.

Notes

The authors declare no competing financial interest.

■ ACKNOWLEDGMENTS

The authors thank Dr Maria Kollia from the Lab of Electron Microscopy and Microanalysis at the University of Patras for the TEM images and the Advanced Light Microscopy Facility of the Department of Physiology, School of Medicine, University of Patras and especially Professor Stavros Taraviras for his help with confocal microscopy.

■ REFERENCES

(1) Boyle, R. G.; Travers, S. Hypoxia: targeting the tumour. *Anti-Cancer Agents Med. Chem.* **2006**, *6*, 281−286.

(2) Huang, J.; Li, Y.; Orza, A.; Lu, Q.; Guo, P.; Wang, L.; Yang, L.; Mao, H. Magnetic Nanoparticle Facilitated Drug Delivery for Cancer Therapy with Targeted and Image-Guided Approaches. *Adv. Funct. Mater.* **2016**, *26*, 3818−3836.

(3) Assaraf, Y. G.; Leamon, C. P.; Reddy, J. A. The folate receptor as a rational therapeutic target for personalized cancer treatment. *Drug Resist. Updates* **2014**, *17*, 89−95.

(4) Boogerd, L. S. F.; Boonstra, M. C.; Beck, A.-J.; Charehbili, A.; Hoogstins, C. E. S.; Prevoo, H. A. J. M.; Singhal, S.; Low, P. S.; van de Velde, C. J. H.; Vahrmeijer, A. L. Concordance of folate receptor-α expression between biopsy, primary tumor and metastasis in breast cancer and lung cancer patients. *Oncotarget* **2016**, *7*, 17442−17454.

(5) Muralidharan, R.; Babu, A.; Amreddy, N.; Bsalingappa, K.; Mehta, M.; Chen, A.; Zhao, Y. D.; Kompella, U. B.; Munshi, A.; Ramesh, R. Folate receptor-targeted nanoparticle delivery of HuR-RNAi suppresses lung cancer cell proliferation and migration. *Nanobiotechnology* **2016**, *14*, 1−17.

(6) Jo, S. D.; Ku, S. H.; Won, Y.-Y.; Kim, S. H.; Kwon, I. C. Targeted Nanotheranostics for Future Personalized Medicine: Recent Progress in Cancer Therapy. *Theranostics* **2016**, *6*, 1362−1377.

(7) Zoppellaro, G.; Kolokithas-Ntoukas, A.; Polakova, K.; Tucek, J.; Zboril, R.; Loudos, G.; Fragogeorgi, E.; Diwoky, C.; Tomankova, K.; Avgoustakis, K.; Kouzoudis, D.; Bakandritsos, A. Theranostics of Epitaxially Condensed Colloidal Nanocrystal Clusters, through a Soft Biomineralization Route. *Chem. Mater.* **2014**, *26*, 2062−2074.

(8) Sarigiannis, Y.; Kolokithas-Ntoukas, A.; Beziere, N.; Zboril, R.; Papadimitriou, E.; Avgoustakis, K.; Lamprou, M.; Medrikova, Z.; Rousalis, E.; Ntziachristos, V.; Bakandritsos, A. Synthesis and evaluation of condensed magnetic nanocrystal clusters with in vivo multispectral optoacoustic tomography for tumour targeting. *Biomaterials* **2016**, *91*, 128−139.

(9) Medříková, Z.; Novohradsky, V.; Zajac, J.; Vrana, O.; Kasparkova, J.; Bakandritsos, A.; Petr, M.; Zboril, R.; Brabec, V. Enhancing Tumor Cell Response to Chemotherapy through the Targeted Delivery of Platinum Drugs Mediated by Highly Stable, Multifunctional Carboxymethylcellulose-Coated Magnetic Nanoparticles. *Chem. - Eur. J.* **2016**, *22*, 9750−9759.

DOI: 10.1021/acsomega.9b03594
ACS Omega 2019, 4, 22214−22227

(10) Bakandritsos, A.; Papagiannopoulos, A.; Anagnostou, E. N.; Avgoustakis, K.; Zboril, R.; Pispas, S.; Tucek, J.; Ryukhtin, V.; Bouropoulos, N.; Kolokithas-Ntoukas, A.; Steriotis, T. A.; Keiderling, U.; Winnefeld, F. Merging High Doxorubicin Loading with Pronounced Magnetic Response and Bio-repellent Properties in Hybrid Drug Nanocarriers. *Small* **2012**, 1−13.
(11) Maeda, H.; Bharate, G. Y.; Daruwala, J. Polymeric drugs for efficient tumor-targeted drug delivery based on EPR-effect. *Eur. J. Pharm. Biopharm.* **2009**, *71*, 409−419.
(12) Angelopoulou, A.; Voulgari, E.; Kolokithas-Ntoukas, A.; Bakandritsos, A.; Avgoustakis, K. Magnetic nanoparticles for the delivery of dapagliflozin to hypoxic tumors: physicochemical characterization and cell studies. *AAPS PharmSciTech* **2018**, *19*, 621−633.
(13) Angelopoulou, A.; Kolokithas-Ntoukas, A.; Papaioannou, L.; Kakazanis, Z.; Khoury, N.; Zoumpourlis, V.; Papatheodorou, S.; Kardamakis, D.; Bakandritsos, A.; Hatziantoniou, S.; Avgoustakis, K. Canagliflozin-loaded magnetic nanoparticles as potential treatment of hypoxic tumors in combination with radiotherapy. *Nanomedicine* **2018**, 2435−2454.
(14) Cao, S.; Slack, S. D.; Levy, C. N.; Hughes, S. M.; Jiang, Y.; Yogodzinski, C.; Roychoudhury, P.; Jerome, K. R.; Schiffer, J. T.; Hladik, F.; Woodrow, K. A. Hybrid nanocarriers incorporating mechanistically distinct drugs for lymphatic CD4 + T cell activation and HIV-1 latency reversal. *Sci. Adv.* **2019**, *5*, No. eaav6322.
(15) Gonzalez-Fajardo, L.; Mahajan, L. H.; Ndaya, D.; Hargrove, D.; Manautou, J. E.; Liang, B. T.; Chen, M.-H.; Kasi, R. M.; Lu, X. Reduced in vivo toxicity of doxorubicin by encapsulation in cholesterol-containing self-assembled nanoparticles. *Pharmacol. Res.* **2016**, *107*, 93−101.
(16) Lee, K. Y.; Mooney, D. J. Alginate: properties and biomedical applications. *Prog. Polym. Sci.* **2012**, *37*, 106−126.
(17) Ayubi, M.; Karimi, M.; Abdpour, S.; Rostamizadeh, K.; Parsa, M.; Zamani, M.; Saedi, A. Magnetic nanoparticles decorated with PEGylated curcumin as dual targeted drug delivery: Synthesis, toxicity and biocompatibility study. *Mater. Sci. Eng., C* **2019**, *104*, No. 109810.
(18) Huang, J.; Li, Y.; Orza, A.; Lu, Q.; Guo, P.; Wang, L.; Yang, L.; Mao, H. Magnetic Nanoparticle Facilitated Drug Delivery for Cancer Therapy with Targeted and Image-Guided Approaches. *Adv. Funct. Mater.* **2016**, *26*, 3818−3836.
(19) Ulbrich, K.; Bakandritsos, A.; Tucek, J.; Zboril, R.; et al. Targeted Drug Delivery with Polymers and Magnetic Nanoparticles: Covalent and Noncovalent Approaches, Release Control, and Clinical Studies. *Chem. Rev.* **2016**, *116*, 5338−5431.
(20) Lim, E. K.; Huh, Y. M.; Yang, J.; Lee, K.; Suh, J.-S.; Haam, S. pH-Triggered Drug-Releasing Magnetic Nanoparticles for Cancer Therapy Guided by Molecular Imaging by MRI. *Adv. Mater.* **2011**, *23*, 2436−2442.
(21) Peng, N.; Wu, B.; Wang, L.; He, W.; Ai, Z.; Zhang, X.; Wang, Y.; Fan, L.; Ye, Q. High drug loading and pH-responsive targeted nanocarriers from alginate-modified SPIONs for anti-tumor chemotherapy. *Biomater. Sci.* **2016**, *4*, 1802−1813.
(22) Afzalipour, R.; Khoei, S.; Khoee, S.; Shirvalilou, S.; Raoufi, N. J.; Motevalian, M.; Karimi, M. R. Dual-Targeting Temozolomide Loaded in Folate-Conjugated Magnetic Triblock Copolymer Nanoparticles to Improve the Therapeutic Efficiency of Rat Brain Gliomas. *ACS Biomater. Sci. Eng.* **2019**, *5*, 6000−6011.
(23) Yan, L.; Luo, L.; Amirshaghaghi, A.; Miller, J.; Meng, C.; You, T.; Busch, T. M.; Tsourkas, A.; Cheng, Z. Dextran-Benzoporphyrin Derivative (BPD) Coated Superparamagnetic Iron Oxide Nanoparticle (SPION) Micelles for T2-Weighted Magnetic Resonance Imaging and Photodynamic Therapy. *Bioconjugate Chem.* **2019**, 2974.
(24) Rasekh, M.; Ahmad, Z.; Cross, R.; Hernandez-Gil, J.; Wilton-Ely, J. D. E. T.; Miller, P. W. Facile Preparation of Drug-Loaded Tristearin Encapsulated Superparamagnetic Iron Oxide Nanoparticles using Coaxial Electrospray Processing. *Mol. Pharmaceutics* **2017**, *14*, 2010−2023.
(25) Martynenko, I. V.; Kusic, D.; Weigert, F.; Stafford, S.; Donnelly, F. C.; Evstigneev, R.; Gromova, Y.; Baranov, A. V.; Ruhle, B.; Kunte, H.-J.; Gun'ko, Y. K.; Resch-Genger, U. Magneto-Fluorescent Microbeads for Bacteria Detection Constructed from Superparamagnetic Fe3O4 Nanoparticles and AIS/ZnS Quantum Dots. *Anal. Chem.* **2019**, *91*, 12661−12669.
(26) Ferjaoui, Z.; Al Dine, E. J.; Kulmukhamedova, A.; Bezdetnaya, L.; Chang, C. S.; Schneider, R.; Mutelet, F.; Mertz, D.; Begin-Colin, S.; Quiles, F.; Gaffet, E.; Alem, H. Doxorubicin-Loaded Thermoresponsive Superparamagnetic Nanocarriers for Controlled Drug Delivery and Magnetic Hyperthermia Applications. *ACS Appl. Mater. Interfaces* **2019**, *11*, 30610−30620.
(27) Zuvin, M.; Kuruoglu, E.; Kaya, V. O.; Unal, O.; Kutlu, O.; Acar, H. Y.; Gozuacik, D.; Kosar, A. Magnetofection of Green Fluorescent Protein Encoding DNABearingPolyethyleneimine-Coated Superparamagnetic Iron Oxide Nanoparticles to Human Breast Cancer Cells. *ACS Omega* **2019**, *4*, 12366−12374.
(28) Alhasan, A. H.; Fardous, R. S.; Alsudir, S. A.; Majrashi, M. A.; Alghamdi, W. M.; Alsharaeh, E. H.; Almalik, A. M. Polymeric Reactor for the Synthesis of Superparamagnetic-Thermal Treatment of Breast Cancer. *Mol. Pharmaceutics* **2019**, *16*, 3577−3587.
(29) Bucak, S.; Yavuzturk, B.; Demir Sezer, A. Magnetic Nanoparticles: Synthesis, Surface Modifications and Application in Drug Delivery. In *Recent Advances in Novel Drug Carrier Systems*, Open access peer-reviewed chapter (paragraph 2 Toxicity); IntechOpen, 2012.
(30) Kato, Y.; Ozawa, S.; Miyamoto, C.; Maehata, Y.; Suzuki, A.; Maeda, T.; Baba, Y. Acidic extracellular microenvironment and cancer. *Cancer Cell Int.* **2013**, *13*, 1−8.
(31) Huang, Y.; Mao, K.; Zhang, B.; Zhao, Y. Superparamagnetic iron oxide nanoparticles conjugated with folic acid for dual target-specific drug delivery and MRI in cancer theranostics. *Mater. Sci. Eng., C* **2017**, *70*, 763−771.
(32) Allard-Vannier, E.; Hervé-Aubert, K.; Kaaki, K.; Blondy, T.; Shebanova, A.; Shaitan, K. V.; Ignatova, A. A.; Saboungi, M.-L.; Feofanov, A. V.; Chourpa, I. Folic acid-capped PEGylated magnetic nanoparticles enter cancer cells mostly via clathrin-dependent endocytosis. *Biochim. Biophys. Acta, Gen. Subj.* **2017**, *1861*, 1578−1586.
(33) Le, T. T. H.; Bui, T. Q.; Ha, T. M. T.; Le, M. H.; Pham, H. N.; Ha, P. T. Optimizing the alginate coating layer of doxorubicin-loaded iron oxide nanoparticles for cancer hyperthermia and chemotherapy. *J. Mater. Sci.* **2018**, *53*, 13826−13842.
(34) Deok Kong, S.; Zhang, W.; Lee, J. H.; Choi, C.; Khamwannah, J.; Karin, M.; Jin, S. Externally triggered on-demand drug release and deep tumor penetration. *J. Vac. Sci. Technol., B: Microelectron. Process. Phenom.* **2012**, *30*, No. 02C102.
(35) Babincová, M.; Altanerov, V.; Altaner, C.; Bergermann, C.; Babinec, P. In vitro analysis of cisplatin functionalized magnetic nanoparticles in combined cancer chemotherapy and electromagnetic hyperthermia. *IEEE Trans. NanoBiosci.* **2008**, *7*, 15−19.
(36) Peiris, P. M.; Bauer, L.; Toy, R.; Tran, E.; Pansky, J.; Doolittle, E.; Schmidt, E.; Hayden, E.; Mayer, A.; Keri, R. A.; Griswold, M. A.; Karathanasis, E. Enhanced delivery of chemotherapy to tumors using a multicomponent nanochain with radio-frequency-tunable drug release. *ACS Nano* **2012**, *6*, 4157−4168.
(37) Pilco-Ferreto, N.; Calaf, G. M. Influence of doxorubicin on apoptosis and oxidative stress in breast cancer cell lines. *Int. J. Oncol.* **2016**, *49*, 753−762.
(38) Zhao, P.; Chen, B.; Li, L.; Wu, H.; Li, Y.; Shaneen, B.; Zhan, Xi.; Gu, N. Missing-in-metastasis protein promotes internalization of magnetic nanoparticles via association with clathrin light chain and Rab7. *Biochim. Biophys. Acta, Gen. Subj.* **2019**, *1863*, 502−510.
(39) Mosmann, T. Rapid colorimetric assay for cellular growth and survival: Application to proliferation and cytotoxicity assays. *J. Immunol. Methods* **1983**, *65*, 55−63.

DOI: 10.1021/acsomega.9b03594
ACS Omega 2019, 4, 22214−22227